

Transient Effects in Intermittently Heated Buildings-Measurements Versus Calculation

Armin TESKEREDŽIĆ, Rejhana BLAŽEVIĆ*, Nijaz DELALIĆ

Abstract: Transient effects in the buildings energy balance are very important and could be dominant in some cases, especially for long setback schedule in the heating system operation. Thermal behaviour of insulated and intermittently heated buildings requires advanced calculation tools for proper estimation of the room/building heat balance. This is especially important for buildings where the heating system is on for up to 10 hours per day. In these buildings the transient effects are dominant and inner walls, due to their significant thermal capacity, strongly influence the variation of the room air temperature in time. In this paper inner walls are divided into side and top/bottom walls and are modelled with transient heat conduction equation each, instead of lumped-thermal-capacity method. Model for simulation is made by using Modelica Buildings Library in Dymola environment. Temperature measurements are recorded in one representative room and measured values are compared with results of simulation. Two cases are analyzed, one with variation of the air room temperature when the thermal inertia of the inner walls is taken into account, and the other where this effect is neglected. The results showed significant variation of the room temperature in the case where heat exchange between the inner walls and room air is neglected compared to the case where thermal inertia of the inner walls is taken into consideration. In case with no influence of the inner walls, due to small thermal inertia of the room air, the analyzed room overheats up to 27 °C during the heating period, while it drops to 9 °C when the heating system is off. Also, internal wall heat fluxes from and towards the room are quantified and analyzed for situations when the heating system is on and is off. It is shown that, for massive and thermally insulated buildings, these heat fluxes can be dominant in the room heat exchange.

Keywords: intermittent heating; inner walls; Modelica; simulation; thermal inertia

1 INTRODUCTION

Current energy policies of the European Union Member States (EU-MS) are focusing on five dimensions [1] among which energy efficiency is one of the key instruments for achieving the goals. According to the world statistics data 40% of energy is used in buildings and therefore the focus is put on long-term programs for refurbishment of existing buildings [2], targeting the cost-optimal solutions of refurbishment and establishing more strict standards for the energy performance of new buildings [3]. As the energy need in buildings is decreasing, mostly as a result of thermal envelope refurbishments, the heating systems are challenged to meet the new working conditions. When the heating system operates for 24 hours per day, the transient effects are negligible but if the intermittent heating is applied, these effects become important and cannot be ignored. This paper deals with transient analysis of the radiator heating and the special role of the thermal inertia of inner walls for intermittently heated massive buildings with low energy need. Previous work focused on different heat transfer mechanisms and cover comprehensive elements of the heat exchange in the rooms [4-10] or provide the software tools for calculation of energy consumption in the heating/cooling season by taking into account transient effects [11].

Potential of thermal energy storage in residential buildings is, also, recognized in district heating systems. Analysis conducted by Kensby et al. [12] showed that building thermal inertia can be utilized for thermal energy storage. Analysis was conducted for five multifamily residential buildings where delivered heat and indoor temperature in one representative room were measured. The obtained results in Kensby et al. indicated that massive buildings can tolerate relatively large variations in heat deliveries while still maintaining a good indoor climate. Research has shown that thermal energy storage is one of the ways for lowering the heating demand without disturbing thermal comfort in buildings.

D'Orazi et al. [13] investigated influence of thermal inertia in the roof slabs on the comfort indoors. An experiment on a full-scale building with different roofs and different climatic conditions was conducted for that purpose. It was noticed that a certain thermal inertia in the slab provides better indoor comfort in both summer and winter. Briga Sá et al. [14] described the influence of the massive wall material, thickness and ventilation system on the Trombe wall thermal performance. It has been demonstrated that during the heating season, for the non-ventilated Trombe wall, the global heat gains decrease is not proportional to the thickness increase. They have stated that this ratio depends on the massive wall material heat storage capacity.

Gracia and Cabeza [15] analyzed thermal energy storage in buildings using sensible, latent heat and thermochemical energy storage. Kumar et al. [16] investigated the thermal performance of phase change material integration in building walls. Also, benefits of applying thermal energy storage in district heating systems to decrease heat load variations were investigated in Romanchenko et al. [17]. In this work a comparison for heat storage using a hot water tank and the thermal inertia of buildings was made.

Heier et al. [18] investigated the combination of thermal energy storage with buildings where a comprehensive review of a wide variety of thermal energy storage technologies is given, with a clear focus on the combination of storage technology and building type. This paper focuses on the influence of inner walls on the room heat balance analysis and uses the model developed in the Modelica Buildings Library [19]. Simulation results are then compared for field measurements results for verification.

Inner walls especially in massive buildings present large heat reservoirs and they can have a huge influence on room temperature distribution in time. Therefore, dynamic building simulation tools play an increasingly important role in planning and sizing the heating systems. By analyzing the transient behavior of the building at various

external and/or internal conditions, dynamic simulation provides a more accurate prediction than the standard engineering tools for system design purposes. In many cases where the energy consumption in buildings is analyzed, the whole building is represented by a couple of typical rooms belonging to the different thermal zones or in some cases a single representative room is chosen for the whole building.

2 ROOM TEMPERATURE MEASUREMENTS AND ANALYSIS OF RESULTS

Test room is carefully selected so that the problems elaborated in this paper can be highlighted, quantified and analyzed. The observed room is placed in the middle of the building, neighboring all heated spaces except one outer surface with windows and a parapet wall exposed to the environment.

Energy efficiency measures were implemented in the building: outside walls were thermally insulated, old windows were replaced and new condensing boiler was installed. The heating system is designed as a single zone, two-pipe system, with central weather compensated control. There are no thermostatic valves at radiators and the water flow in the distribution system is constant, independently from the variations of the outside temperature.

The heating system operates for 9 hours per day during weekdays with a special program over the weekends (three hours of heating on Saturdays and one hour on Sundays), again irrespective of the outside temperatures. During the working week, system starts at 6 AM and it works until 3 PM. The period when the system is off is quite long, especially after the weekend, causing the sub-cooling of the inner walls which at the end affects the room heat balance significantly. In this case the transient effects become important and the standard approach of steady-state calculations for room heat balance are practically useless. The geometry of the observed room and the position of four temperature sensors TC1 to TC4, their connection to the data logger and a PC for data acquisition are shown in Fig. 1.

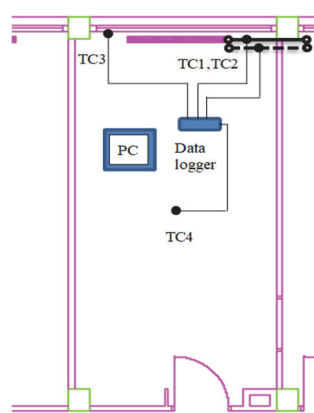


Figure 1 Observed room with measurement scheme

Fig. 2 shows the generic calculation domain with one radiator, one external wall and windows. Size of the room is 7/3,28/3,46 in meters ($W/L/H$), while the outer exposed surface consists of 6 windows and the wall. Total windows

size is $3,00 \times 2,35$ m ($7,05$ m²), while the outside wall covers an area of $4,33$ m². Radiator is placed at the middle of the outside wall below the windows.

Four column cast iron radiator Jadran 600/4-20 with a nominal power of $\phi_{rad}^N = 3040$ W is installed, corresponding to the standard 90/70/20 °C temperature regime. Vertical supply and return branch pipelines for the observed room are placed in the neighboring room, which excludes additional heating of the observed room that could cause the heat emission of uninsulated distribution pipes.

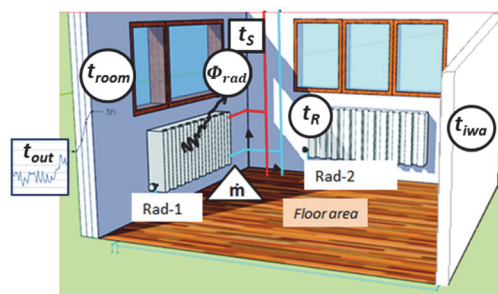


Figure 2 Generic room for in-huse developed calculation tool

The following quantities are measured in the observed room:

- Temperatures at the surface of the supply and return water pipes (Fig. 3).
- Temperature of the inner surface of the outer wall (Fig. 4).
- Room air temperature (Fig. 5).



Figure 3 Temperature measurement at supply and return pipes

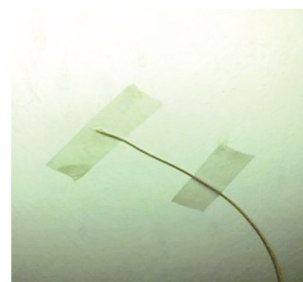


Figure 4 Temperature measurement of the inner surface of the outer wall

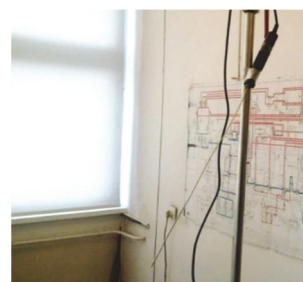


Figure 5 Room air temperature measurement

Fig. 3 shows location of sensors TC1 and TC2 connected to the supply and return pipes, which are insulated from the outside in order to reduce the effect of cooling. Measured temperatures are then corrected to get the water supply and return temperatures.

Temperature measurement of the inner surface of the outer wall is done at a height of 0,5 m from the floor level, which is shown in Fig. 4. Finally, Fig. 5 presents the assembly for measurement of the room air temperature, where the sensor TC4 was placed in the middle of the room, on a stand at a height of 1,5 meters from the floor level according to recommendations.

The temperature sensor signals were collected with the four-channel data logger for temperature measurements with K-type thermocouples, as shown in Fig. 6. Data Logger is connected to the laptop (Fig. 7) where measurements data are recorded and monitored.



Figure 6 Four channel data logger



Figure 7 Data logger connection to laptop for data acquisition

Measurements with sensors TC1 to TC4 were performed in a one-minute interval during 36 hours, covering one and a half full heating cycle. Values are recorded starting from the point where the heating system was switched off. At that moment the time was set to zero and this fact is used in graphical representation of results. In addition to described measurements, the outside air temperature values were taken from the existing building energy management and monitoring system. Outside air temperature was measured by a Pt-100 sensor and recorded every hour. Values for the prescribed interval of one minute were calculated by linear interpolation between hourly values.

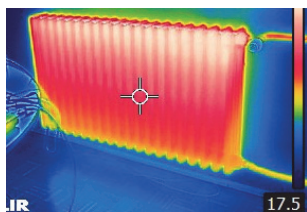


Figure 8 Infrared thermal image of the radiator

For illustration purposes, the qualitative temperature profiles of the radiator and thermal image of windows are made with infrared thermal camera (Fig. 8 and Fig. 9). Measurement of the mass and/or volume flow rate of the water supplying radiator was not done. Mass flow rate at the radiator is estimated using the procedure explained in [20]. As a first guess, the value calculated based on the nominal power of the radiator can be taken.

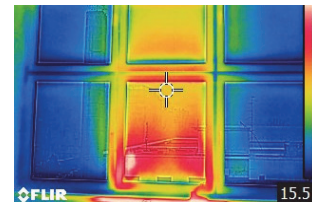


Figure 9 Infrared thermal image of the windows

However, the mass flow rate in the radiator depends on the design concept (fix or variable flow in the distribution network), existence of the thermostatic valves, the level of the hydronic balancing in the network, available differential pressures and these facts may bring additional difficulties for the mass flow rate estimation. Based on the experience from the field, the situation in which perfect hydronic balancing is obtained which results in nominal flow through the radiator is almost impossible to find in existing buildings, at least in South East Europe.

In Fig. 10 measured values of supply (red), return (blue) water temperatures and room air temperature (green) are given.

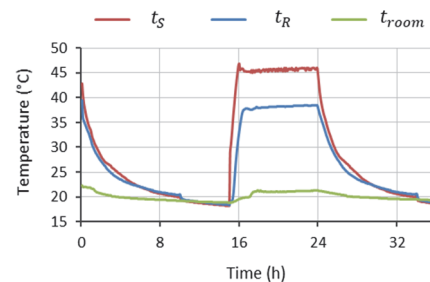


Figure 10 Measured water supply (red), return (blue) and room (green) temperatures

Interpolated outside temperature is presented in Fig. 11. It can be seen that the variation of the outside temperature (-1°C to 3°C) is not significant in the period of measurements and therefore the supply temperature set by weather compensated control is around 45°C (Fig. 10).

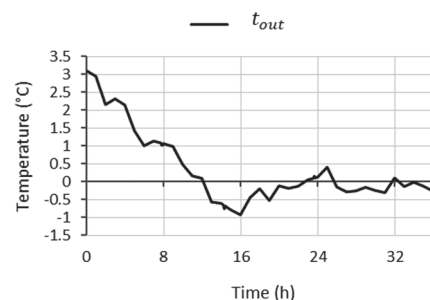


Figure 11 Measured ambient temperature

3 ESTIMATION OF THE MASS FLOW RATE IN RADIATOR

Mass flow rate in the radiator is estimated based on the combination of the nominal power of the radiator and available measured temperatures of the room air and water supply and return as proposed in [20]. One should bear in mind that the heat exchange in the observed room is strongly transient because of the long period when the system is off.

The change of the room air temperature in time is significantly influenced by the thermal inertia of inner walls and partly by the thermal inertia of the radiator (radiator body and its water content). The latter is important when the heating system is switched off. The current procedure requires the steady-state operation at least in one short period of time in order to make correct estimation of the mass flow rate [20].

When the steady-state is reached, the transient term in radiator equation vanishes and the following heat balance for radiator is valid:

$$\dot{m}c(t_S^{st} - t_R^{st}) = \phi_{rad}^N \left(\frac{\Delta t_m}{\Delta t_m^N} \right) \quad (1)$$

where heat flux ϕ_{rad}^N is the nominal power of the radiator, Δt_m and Δt_m^N are the temperature differences between the radiator body and the room temperature in current and nominal conditions, respectively, while n is the radiator exponent.

Left hand side of Eq. (1) is the heat flux which hot water delivers to the radiator body, while the right-hand side presents the heat flux which radiator emits towards the room air.

Fig. 12 shows the radiator heat flux based on measured values and calculated with the help of the right-hand side part of Eq. (1).

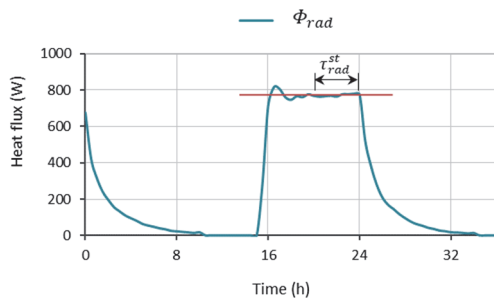


Figure 12 Estimated heat flux from radiator based on measured values

Interval in which the heat flux is stable is marked with τ_{rad}^{st} and its mean value is shown in red line in Fig. 12. For this interval the square flux error function is introduced as:

$$\phi_{err} = \sum_{i=1}^K \left\{ \phi_{rad}^N \left[\frac{0,5(t_S^i - t_R^i) - t_{room}^i}{\Delta t_m^N} \right]^n - \dot{m}c(t_S^i - t_R^i) \right\}^2 \quad (2)$$

where t_S^i , t_R^i and t_{room}^i are measured values of water supply, return and room air temperatures for the i -th time

step, within interval $\tau_{rad}^{st} i = 1$ to K , which is graphically presented in Fig. 13. An error heat flux function is squared and the minimum of this function is sought by varying the mass flow rate.

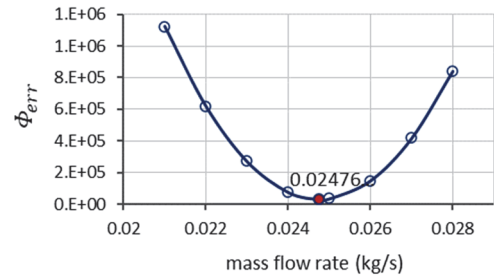


Figure 13 Square of error flux according to Eq. (2)

Fig. 13 shows the functional dependency of the square heat flux error defined by Eq. (2) versus variation of the mass flow rate between 0,021 and 0,028 kg/s. The exact minimum of this function is found by applying halving of intervals numerical method.

Fig. 14 shows the relative error between heat flux values calculated for the left-hand side and the right-hand side of Eq. (1), within prescribed interval and after the mass flow rate is prescribed. The deviation of these two fluxes is not significant especially if one bears in mind that the process within the prescribed period is not fully steady-state and transient term in reality does not disappear completely. At contrary, if the nominal conditions for the radiator are taken as reference for mass flow estimation, the result would be 0,03667 kg/s, which presents the overestimation of the mass flow for 33% and which may lead to additional calculation error.

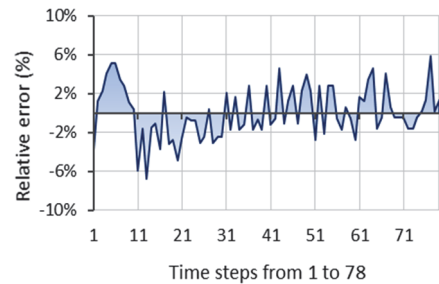


Figure 14 Relative heat flux error for selected time interval

4 MODELICA MODEL AND INITIAL AND BOUNDARY CONDITIONS

Modelica Buildings Library under Dymola environment is used for modeling purposes. Developed In-house calculation models of the room and windows are used and applied for the transient room heat balance. Since $Biot$ numbers for both, side and top/ bottom walls are larger than 0,1 the lumped-thermal-capacity method for modelling of inner walls has not been used. Instead, side and top/bottom inner walls are modelled with 9 nodes each, solving the discretized form of the transient heat conduction equation. At all inner walls an adiabatic boundary condition was applied at the opposite side of the room, assuming that the neighboring rooms have identical temperature variation in time as the observed one. Therefore, only one half of the inner walls thickness is

taken in the calculation domain which makes the definition of adiabatic boundary condition at their opposite side – justified.

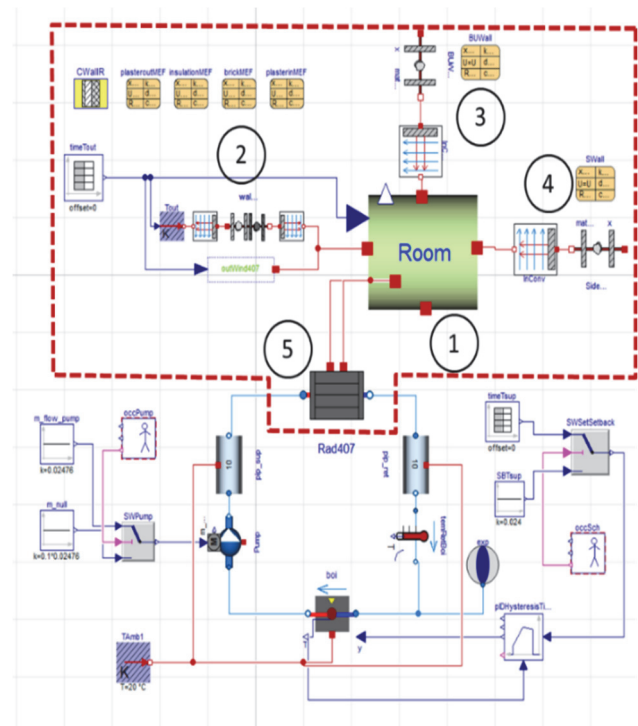
With intention to demonstrate the applicability of the Modelica Buildings Library model, the heating system with its control is also modelled (Fig. 15). Variables in the rectangular boxes in Fig. 2 were known values, which were used as input parameters in the simulation. These are t_{out} as an ambient or outside air temperature and t_s as the radiator supply temperature. One may notice that the mass flow in the radiator \dot{m} is shown in a triangle, since its value has to be known as an input parameter as well. The mass flow rate calculation is explained in the previous subsection and obtained value is used in calculation. Variables presented in circles in Fig. 2, such as t_{room} as room air temperature, Φ_{rad} as the radiator heat flux, t_{iwa} as an average internal walls temperature, and t_R as the return water temperature are unknown variables and are the output values of the simulation.

Note that for simplification purposes, two different values of inner walls temperatures bottom and top inner walls temperature at one side, and side inner walls temperature at the other side, are represented with average internal walls temperature t_{iwa} .

The following assumptions are used to model the room heat balance. A room air is presented with one computational control volume, which implies uniform room air temperature over its volume. The radiator body is divided into 20 control volumes and the thermal mass of radiator body is lumped into the water content for each volume. Outer walls are made of 4 different materials and this part of the domain is discretized into 12 control volumes for which the transient conduction equation is solved. Equations for radiator, outside walls, windows, inner walls and the boiler with distribution system are implicitly coupled and provide results of all unknown variables at any instant of time.

Thermo-physical properties of 4 different layers of the outer wall are given in the Tab. 1. Initial room temperature is set as 22,3 °C and initial inner wall temperature is set to 19 °C, both measured at the start of the measurement. It is assumed that convective heat transfer coefficients are 8 W/m²K and 20 W/m²K at inner and outer side of outside

walls, respectively. Inner walls consist of top and bottom area of 45,9 m² while side inner walls cover the area of 59,8 m², with convective heat transfer coefficients of 3 W/m²K and 6 W/m²K, respectively. Heat transfer coefficient for windows is $U_{win} = 1,4 \text{ W/m}^2\text{K}$.



Legend: 1 Room model*, 2 Outside composite wall and windows, 3 Bottom and top inner walls, 4 Side inner walls, 5 Radiator
Subdomain in red dashed line relevant for comparison of calculation vs measurements
*Includes infiltration of outside air and allows connection to all walls and radiator via heat ports

Figure 15 Modelica Buildings Model in Dymola and subdomain relevant for calculation in red dashed marked region

Thermo-physical properties of the side and bottom and top walls are given in Tab. 2. Note that only half of the thickness of these layers is taken into account. This is because of the adiabatic boundary conditions applied at opposite boundaries to the room, assuming that all rooms neighboring the observed room have identical temperature.

Table 1 Thermo-physical properties of outer wall

Layer	Material	Thickness / m	Thermal conductivity / W/mK	Specific heat / J/kgK	Density / kg/m ³
1.	Cement mortar	0,02	1,4	1000	1800
2.	EPS	0,1	0,04	1450	20
3.	Hollow brick	0,25	0,64	900	1600
4.	Lime mortar	0,02	0,81	1000	1500

Table 2 Thermo-physical properties of inner walls

Material	Thickness / m	Thermal conductivity / W/mK	Specific heat / J/kgK	Density / kg/m ³
Side walls brick	0,08	0,68	1600	900
Bottom/Top concrete	0,10	2,50	1000	2400

Initial outer wall temperature is obtained from steady-state condition by taking available initial outside and inside temperatures. Initial temperature of radiator is taken as an arithmetic average of supply and return temperatures at the start of measurements. Total water volume in radiators is 32 l, unit mass of empty radiator is 134 kg with specific heat 500 J/kgK used in calculations.

Boundary conditions necessary to close the problem are defined by the outside temperature and heating system

water supply temperature, both available during the whole period of measurements. Note that the distribution system in Modelica model is modelled with no thermal losses in the distribution system which coupled with an ideal control of the boiler exit temperature, resulted in perfect agreement with measured water supply temperature entering the radiator.

5 RESULTS AND DISCUSSION

In this section the obtained results are analyzed and compared with measured data. On top of that, the heat exchange between inner walls and room air is discussed and quantified. Simulation results provide values of unknown variables such as: room temperature (t_{room}), radiator heat flux (Φ_{rad}), return hot water temperature (t_R) and inner walls temperature (t_{iwa} as averaged side and top and bottom inner walls temperature) at any instant of time. Calculated values t_{room} , Φ_{rad} , t_R are compared with measured values, while the temperature of inner walls t_{iwa} is also presented and discussed, although not measured in this case.

The comparison of measured and calculated room air temperatures is shown in Fig. 16. There is a good agreement which indicates that the initial inner walls temperatures are correctly guessed and t_{iwa} is also presented at the graph with dashed black line. It can be seen that the variation of the air room temperature is more intensive than the temperature variation of the inner walls because of the high thermal inertia of the inner walls compared to thermal inertia of the room air. Also, it can be seen that the room air temperature drops faster within first calculation period because of the larger temperature gradient between the room air and inner walls. At one instant of time the room air temperature drops below the inner wall's temperature and in this region the variation of the room temperature is lower due to the fact that inner walls provide heat gains towards room air. The heat flux sign changes and inner walls from that moment onwards make a positive contribution to the room heat balance.

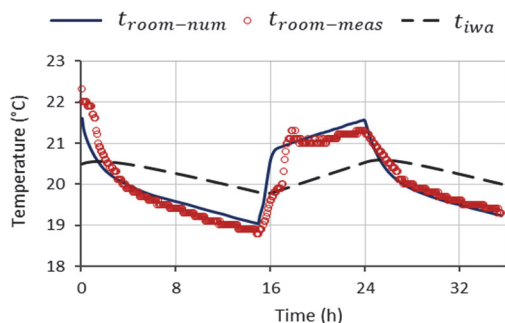


Figure 16 Measured vs. calculated room air temperature with thermal inertia of inner walls

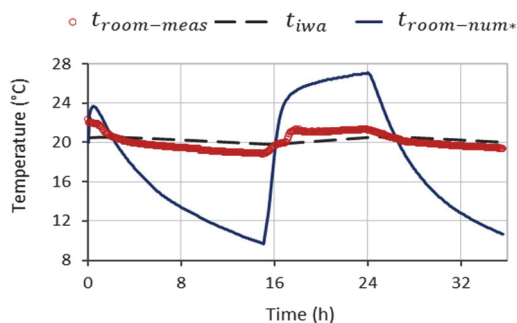


Figure 17 Measured vs. calculated room air temperature without thermal inertia of inner walls

Fig. 17 shows the calculated case with the same initial and boundary conditions but with no influence of the inner walls convective heat transfer coefficients are set to zero at

all inner walls. It means that heat exchange between the inner walls and room air is neglected in this case. It is obvious that due to small thermal inertia of the room air, the variation of the room temperature is significant, the room overheats up to 27 °C during the heating period, while it drops to 9 °C when the heating system is off.

Fig. 18 provides the comparison of calculated and measured values of the return water temperature. The agreement between measured and calculated results is excellent. This is the proof that the mass flow in the radiator is correctly estimated by the proposed approach elaborated by using Eq. (2) and as shown in Fig. 13. Also, in the period when the heating system is off, again very good agreement between calculated and measured return temperature values is recognized. It means that the physical properties of the radiator are correct, since in this period there is no flow in the radiator and the heat flux from the radiator is only due to the cooling of the trapped hot water in the radiator, including the radiator body.

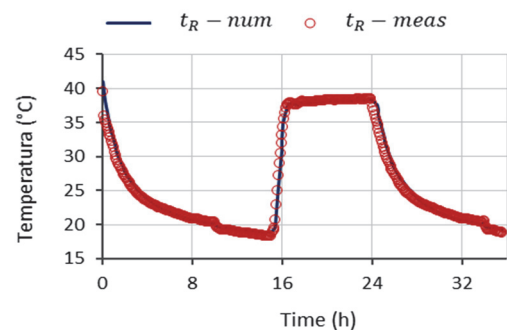


Figure 18 Calculated vs. measured values of water return temperature

Calculated and estimated heat fluxes from the radiator are shown in Fig. 19. Again, very good agreement can be noticed which is the result of correct estimation of the return temperature, correct mass flow and good estimation of the room air temperature.

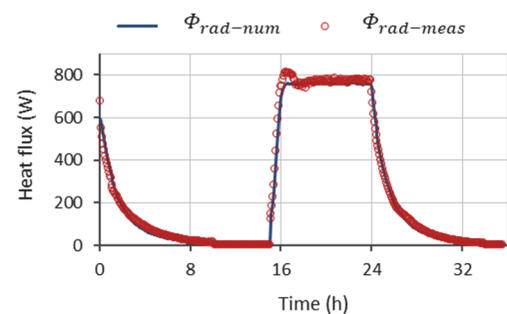


Figure 19 Calculated vs. estimated values of radiator heat flux

Proposed methodology converts the original three-dimensional problem (3D) into one dimensional and 3D effects are neglected consequently. However, the major effects of transient radiator room heating are properly evaluated by the calculations and it is of utmost importance to underline the influence of the inner walls on the overall room heat balance.

Inner walls can be interpreted as the heat reservoir in the room, which is dumping the large variation of the room air temperature, demonstrated in Fig. 20 and Fig. 21. Fig. 20 shows the incoming heat flux from radiator Φ_{rad} (red

line) and the alternating heat flux from (positive) and towards the inner walls Φ_{iwa} (negative) is presented with blue area.

It can be seen that when the heating system is off, a major positive contribution or the heat gain comes from the inner walls. The physical interpretation is that within this period the room temperature goes down faster and the inner walls due to significantly larger thermal inertia are warmer than the room air. At contrary, when the heating system is on, again as a result of small thermal inertia of the room air, the room temperature increases faster and at some stage room air becomes warmer than inner walls which implies that inner walls become a heat sink. From that moment onwards the heat flux Φ_{iwa} changes its sign and it is directed from the room air towards inner walls.

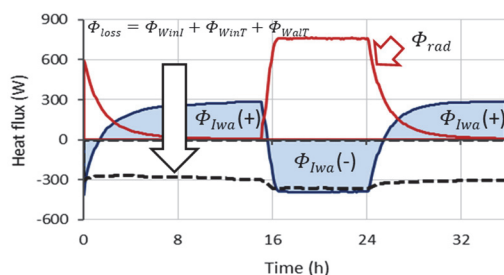


Figure 20 Heat gains versus heat losses for calculation period

In Fig. 21 (top) the ratios of the single heat flux components are presented when the heating system is on. It can be seen that more than a half of the total heat gains from the radiators is 'spent' on inner walls. The rest covers the heating of the room air and on compensation of the transmission and infiltration losses (Φ_{WalT} , Φ_{WinT} , Φ_{WinI}) via outer walls and windows. In Fig. 21 (bottom) at the instant of time when radiators are almost cooled at the room temperature (heating system is off), most of the heat gain towards room air comes from inner walls as a partial compensation of transmission and infiltration losses. Note that if the heat losses over the heat gains prevail (system is off), the room temperature decreases and vice versa.

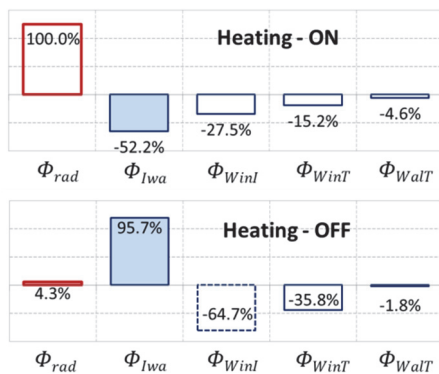


Figure 21 Redistribution of relative gains and losses

In general, the inner walls can be treated as heat sinks when the heating system is on, since the room temperature is larger than the inner walls temperature and the heat flux is directed from the room towards inner walls. At contrary, when the heating system is off, the inner walls are playing the role of the heat source because of the larger inner wall temperature in comparison with room temperature and the

heat flux is in the opposite direction. The fact is that inner walls are playing important role in damping the strong variation of the room air temperature due to their large thermal inertia.

6 CONCLUSIONS AND FURTHER WORK

Energy efficient programs of refurbishment of existing buildings are expanding in the region of South East Europe. In some cases, only preliminary and very simple calculation tools are used to justify the feasibility of these measures. However, envelope refurbishments are introducing new challenges and impose more strict conditions for the heating systems control and smooth operation. This is especially valid for massive buildings with intermittent heating. This paper shows that if the periods of heating are shorter than the periods when the system is in setback or off, the transient effects are prevailing and the inner walls influence become very important, if not dominant, in the room heat balance. Existing calculation tools for engineers in most cases do not take this phenomenon into account and the problems during exploitation may occur. If estimated heat losses take into account only transmission and infiltration/ventilation losses, the required heat flux from radiators will be underestimated. Consequently, the supply temperature settings for weather compensated control will be wrong as well which may lead to problems with thermal comfort. This paper focuses on the importance of proper handling of inner walls influence and provides both: measurements and model and simulation with advanced modelling tool. The results showed that, when the heating system is on, inner walls with their large thermal inertia represent a heat sink which means that more than 50% of the total heat gains from the radiators is spent for heating of inner walls. Also, when the heating system is off, the most of the heat gain towards room air comes from inner walls, almost 96%, which in that case have the role of the heat source. The extension of the developed calculation methodology for 3D constructions by applying CFD tools is in progress and preliminary results are promising.

7 REFERENCES

- [1] Energy Union Package (2015). A Framework Strategy for a Resilient Energy Union with a Forward-Looking Climate Change Policy, EU Commission.
- [2] Directive 2012/27/EU (2012). On energy efficiency (EED) of the European Parliament and of the Council of 25 October 2012.
- [3] Directive 2010/31/EU (2010). Of the European Parliament and of the Council of 19 May 2010 on the energy performance of buildings (EPBD).
- [4] Delcroix, B., Kummert, M., Daoud, A., & Hiller, M. D. (2012). Conduction transfer functions in TRNSYS multizone building model: current implementation, limitations and possible improvements. *Proceedings of SimBuild*, 5(1), 219-226.
- [5] Delcroix, B., Kummert, M., Daoud, A., & Hiller, M. (2013). Improved conduction transfer function coefficients generation in TRNSYS multizone building model. *Proceedings of BS2013, Chambéry, France*, 2667-2674.
- [6] Wetter, M. (2006). Multizone building model for thermal building simulation in modelica. *Proceedings of the 5th International Modelica Conference*, 517-526.

- [7] Wetter, M., Zuo, W., & Nouidui, T. S. (2011). Modeling of heat transfer in rooms in the modelica" buildings" library. *Proceedings of the 12th Conference of International Building Performance Simulation Association*, 1096-1103. <https://doi.org/10.2172/1168737>
- [8] Nouidui, T. S., Phalak, K., Zuo, W., & Wetter, M. (2012). Validation and Application of the Room Model of the Modelica Buildings Library. *Proceedings of the 9th International Modelica Conference*, 727-736. <https://doi.org/10.3384/ecp12076727>
- [9] Felgner, F., Cladera, R., Merz, R., & Litz, L. (2003). Modeling thermal building dynamics with Modelica. *Proceedings of the 4th Mathmod Conference*, 101-109.
- [10] Wetter, M & Haugstetter, C. (2006). Modelica versus TRNSYS-A comparison between an equation-based and a procedural modeling language for building energy simulation. *Proceedings of SimBuild*, 2(1), 262-269.
- [11] Crawley, D. B., Lawrie, L. K., Winkelmann, F. C., Buhl, W. F., Huang, Y. J., Pedersen, C. O., ... & Glazer, J. (2001). EnergyPlus: creating a new-generation building energy simulation program. *Energy and buildings*, 33(4), 319-331. [https://doi.org/10.1016/S0378-7788\(00\)00114-6](https://doi.org/10.1016/S0378-7788(00)00114-6)
- [12] Kensby, J., Trüschel, A., & Dalenbäck, J. O. (2015). Potential of residential buildings as thermal energy storage in district heating systems—Results from a pilot test. *Applied Energy*, 137, 773-781. <https://doi.org/10.1016/j.apenergy.2014.07.026>
- [13] D'Orazio, M., Di Perna, C., & Di Giuseppe, E. (2014). A field study of thermal inertia of roofs and its influence on indoor comfort. *Journal of Building Physics*, 38(1), 50-65. <https://doi.org/10.1177/1744259113480134>
- [14] Briga Sá, A. C., Martins, A., Boaventura-Cunha, J., Carlos Lanzinha, J., & Paiva, A. (2018). An analytical approach to assess the influence of the massive wall material, thickness and ventilation system on the Trombe wall thermal performance. *Journal of Building Physics*, 41(5), 445-468. <https://doi.org/10.1177/1744259117697389>
- [15] De Gracia, A. & Cabeza, L. F. (2015). Phase change materials and thermal energy storage for buildings. *Energy and Buildings*, 103, 414-419. <https://doi.org/10.1016/j.enbuild.2015.06.007>
- [16] Kumar, S., Arun Prakash, S., Pandiyarajan, V., Geetha, N. B., Antony Aroul Raj, V., & Velraj, R. (2020). Effect of phase change material integration in clay hollow brick composite in building envelope for thermal management of energy efficient buildings. *Journal of Building Physics*, 43(4), 351-364. <https://doi.org/10.1177/1744259119867462>
- [17] Romanchenko, D., Kensby, J., Odenberger, M., & Johnsson, F. (2018). Thermal energy storage in district heating: Centralised storage vs. storage in thermal inertia of buildings. *Energy conversion and management*, 162, 26-38. <https://doi.org/10.1016/j.enconman.2018.01.068>
- [18] Heier, J., Bales, C., & Martin, V. (2015). Combining thermal energy storage with buildings—a review. *Renewable and Sustainable Energy Reviews*, 42, 1305-1325. <https://doi.org/10.1016/j.rser.2014.11.031>
- [19] Modelica Buildings Library, See <https://simulationresearch.lbl.gov/modelica/releases/latest/help/Buildings.html>
- [20] Teskeredzic, A. & Blazevic, R. (2018). Transient Radiator Room Heating-Mathematical Model and Solution Algorithm. *Buildings*, 8(11), 1-18. <https://doi.org/10.3390/buildings8110163>

Contact information:

Armin TESKEREDŽIĆ, Dr.sc. Associate Professor
Faculty of Mechanical Engineering Sarajevo,
Vilsonovo šetalište 9, 71000 Sarajevo, Bosnia & Herzegovina
E-mail: teskeredzic@mef.unsa.ba

Rejhana BLAŽEVIĆ, Dr.sc. Assistant Professor
(Corresponding author)
Faculty of Mechanical Engineering Sarajevo,
Vilsonovo šetalište 9, 71000 Sarajevo, Bosnia & Herzegovina
E-mail: muhamedagic@mef.unsa.ba

Nijaz DELALIĆ, MSc.
Faculty of Mechanical Engineering Sarajevo,
Vilsonovo šetalište 9, 71000 Sarajevo, Bosnia & Herzegovina
E-mail: delalic@mef.unsa.ba